J. Fluid Mech. (2020), *vol.* 901, E1.
doi:10.1017/jfm.2020.557

CORRIGENDUM

Global instability in the onset of transonic-wing buffet – CORRIGENDUM

J. D. Crouch, A. Garbaruk and M. Strelets

doi:10.1017/jfm.2019.748, Published online by Cambridge University Press, 24 October 2019

The original paper Crouch, Garbaruk & Strelets (2019) identified three global modes of instability associated with swept-wing buffet: long-wavelength modes, intermediate-wavelength modes, and short-wavelength modes.

Following that earlier investigation, an independent study using an alternative formulation for the stability equations (Paladini *et al.* 2019) was not able to reproduce the growth characteristics for the short-wavelength modes. Meanwhile, we also applied a new formulation based on a fully three-dimensional eigenfunction to independently assess the initial results. In the course of this work, an error was identified in the numerical results by Crouch *et al.* (2019) associated with a term in the eddy-viscosity equation. The error (here corrected) had minimal impact on the frequencies but a larger impact on the growth rates, with the error increasing with the spanwise wave number. While the long-wavelength and intermediate-wavelength growth rates are weakly altered, the short-wavelength growth rates are significantly modified.

Figures 3, 4, 6, and 7, and figures 10 through 14 are replotted here based on the original formulation by Crouch *et al.* (2019) with corrected numerics. The discussion and overall findings by Crouch *et al.* (2019) remain unchanged, with the exception that the peak growth rate for the short-wavelength modes occurs at $\beta \approx 25$ as opposed to $\beta \approx 45$, and the short-wavelength onset of instability is now consistently supercritical to the long-wavelength oscillatory modes. The overall agreement between the stability analysis and the URANS is slightly improved. The new figures provide a quantitative correction to the growth rates and stability boundaries, but are qualitatively the same.

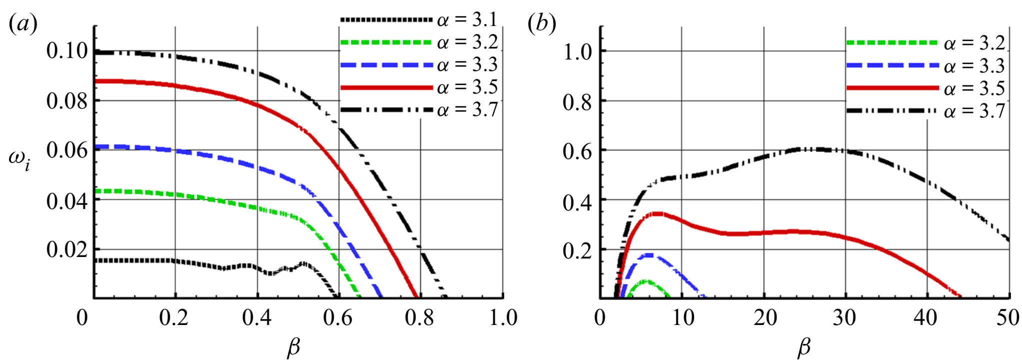

FIGURE 3. Instability growth rates at $M = 0.73$, $Re = 3 \times 10^6$ as a function of β for (*a*) oscillatory modes and (*b*) stationary modes (OAT15A).

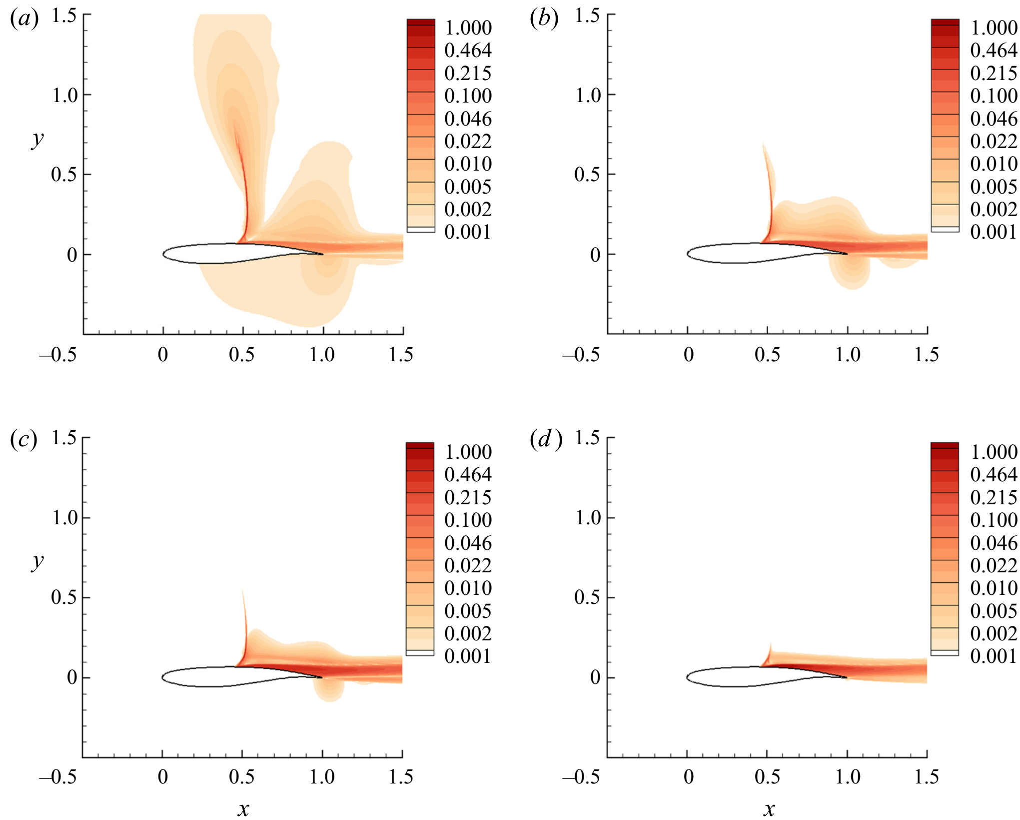

FIGURE 4. Magnitude of u component of instability for $M = 0.73$, $\alpha = 3.6^\circ$, and $Re = 3 \times 10^6$ with different values of β: (*a*) $\beta = 0$ oscillatory, (*b*) $\beta = 6$ stationary, (*c*) $\beta = 12$ stationary, (*d*) $\beta = 45$ stationary (OAT15A).

https://doi.org/10.1017/jfm.2020.557 Published online by Cambridge University Press

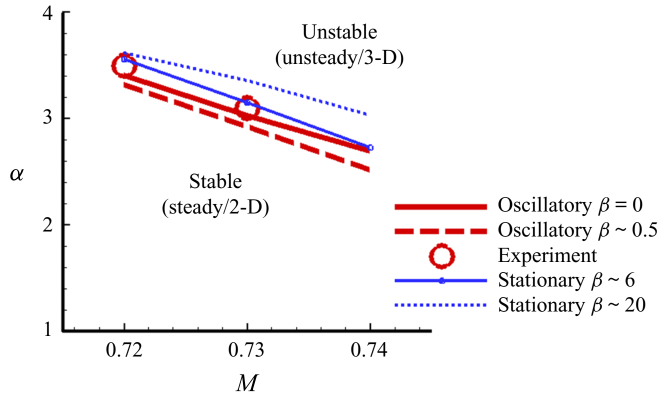

FIGURE 6. Stability boundaries for different β values corresponding to local maxima of the growth rate at $Re = 3 \times 10^6$ (OAT15A).

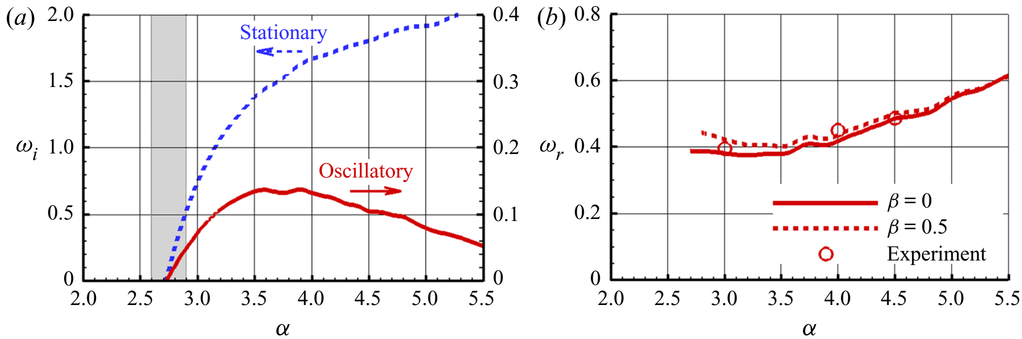

FIGURE 7. Variation with angle of attack for (*a*) growth rates of the stationary and oscillatory modes, and (*b*) oscillatory-mode frequencies for the dominant range of β. Results at $M = 0.73$ and $Re = 3 \times 10^6$ (RA16SC1).

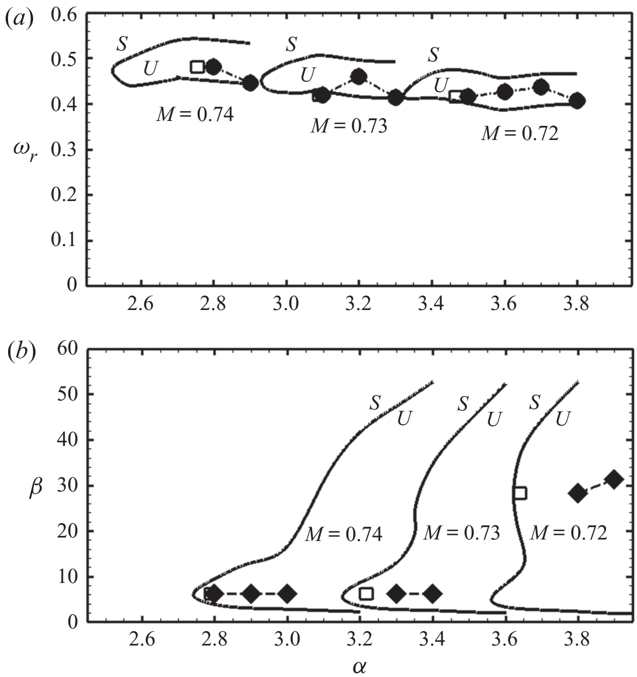

FIGURE 10. Neutral stability curves for (a) oscillatory modes, and (b) stationary modes, with S and U showing stable and unstable regions, respectively. Solid symbols are results from URANS, and open symbols are extrapolated URANS results at instability onset. Results at $M = 0.72, 0.73, 0.74$ and $Re = 3 \times 10^6$ (OAT15A).

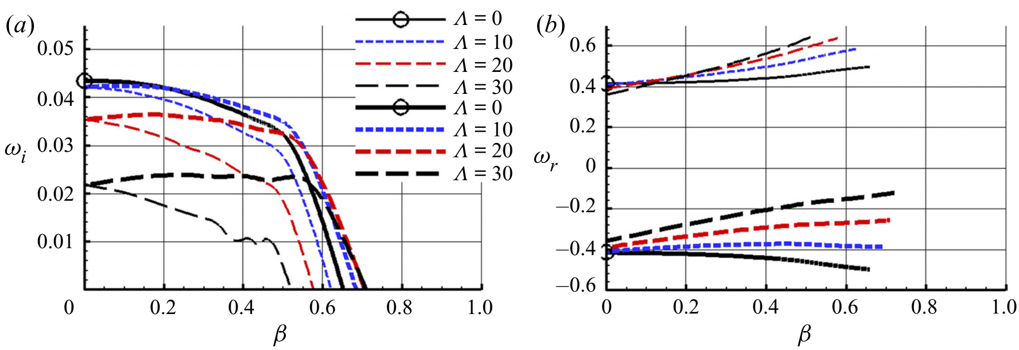

FIGURE 11. Oscillatory mode (a) growth rates and (b) frequencies for different sweep angles $\Lambda = 0°, 10°, 20°, 30°$ at $M_n = 0.73$, $\alpha_n = 3.2°$ and $Re_n = 3 \times 10^6$ (OAT15A).

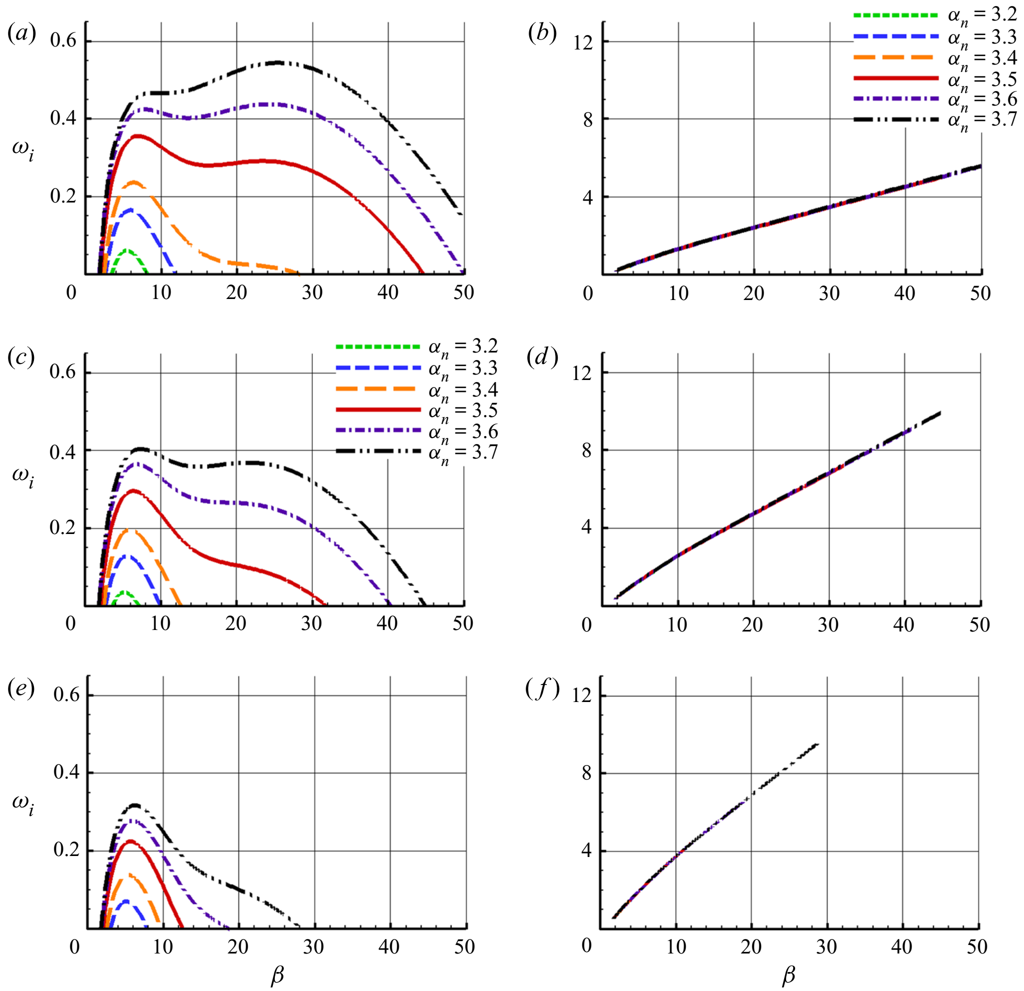

FIGURE 12. Travelling mode growth rate and frequency as a function of β for infinite swept wing with: (*a*,*b*) $\varLambda = 10^{\circ}$, (*c*,*d*) $\varLambda = 20^{\circ}$, (*e*,*f*) $\varLambda = 30^{\circ}$, at $M_n = 0.73$ and $Re_n = 3 \times 10^6$ (OAT15A).

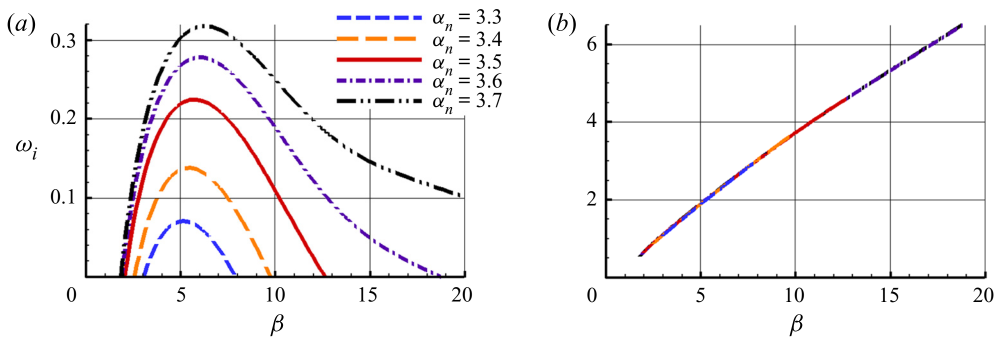

FIGURE 13. Travelling mode (*a*) growth rate and (*b*) frequency as a function of β for $\varLambda = 30^{\circ}$. Results for different values of α_n with $M_n = 0.73$, $Re_n = 3 \times 10^6$ (OAT15A).

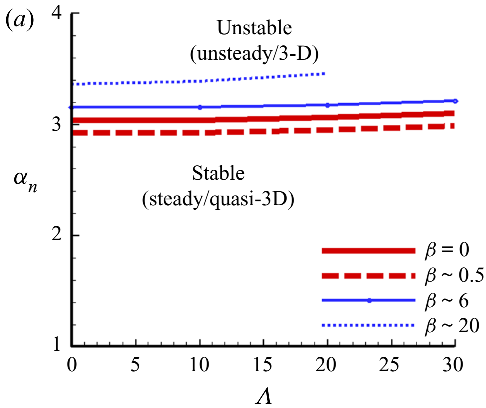

FIGURE 14. Stability boundaries as a function of sweep for different β values corresponding to local maxima of the growth rate. Results in terms of (*a*) α_n and (*b*) α for $M_n = 0.73$ and $Re_n = 3 \times 10^6$ (OAT15A).

Declaration of interests

The authors report no conflict of interest.

REFERENCES

CROUCH, J. D., GARBARUK, A. & STRELETS, M. 2019 Global instability in the onset of transonic-wing buffet. *J. Fluid Mech.* **881**, 3–22.

PALADINI, E., BENEDDINE, S., DANDOIS, J., SIPP, D. & ROBINET, J. CH. 2019 Transonic buffet instability: from two-dimensional airfoils to three-dimensional swept wings. *Phys. Rev. Fluids* **4**, 103906.